Heliyon 9 (2023) e17119

Contents lists available at ScienceDirect

Heliyon

journal homepage: www.cell.com/heliyon

Single-cell transcriptome analysis reveals T population heterogeneity and functions in tumor microenvironment of colorectal cancer metastases

Jing Zhuang [a,b,c,1], Zhanbo Qu [a,b,c,1], Jian Chu [a,b,c,1], Jingjing Wang [a], Yinhang Wu [a,b,c], Zhiqing Fan [a], Yifei Song [a], Shuwen Han [a,b,c], Lixin Ru [a,b,c], Hui Zhao [a,b,c,*]

[a] Huzhou Central Hospital, Affiliated Central Hospital Huzhou University, China
[b] Fifth Affiliated Clinical Medical College of Zhejiang Chinese Medical University, Huzhou Central Hospital, China
[c] Key Laboratory of Multiomics Research and Clinical Transformation of Digestive Cancer of Huzhou, China

ARTICLE INFO

Keywords:
Colorectal cancer
Single-cell RNA sequencing
T cell subset
Immune microenvironments
Immunotherapy

ABSTRACT

Cell mediated immune escape, a microenvironment factor, induces tumorigenesis and metastasis. The purpose of this study was to display the characteristics of T cell populations in immune microenvironments for colorectal cancer (CRC) metastasis. Unsupervised cluster analysis was conducted to identify functionally distinct T cell clusters from 3,003 cells in peripheral blood and 4,656 cells in tissues. Subsequently, a total of 8 and 4 distinct T cell population clusters were identified from tumor tissue and peripheral blood, respectively. High levels of CD8+TEX, CD4+TRM, TH1-like T cells, CD8+TEM, tumor-Treg from tissues, and CD4+TN from peripheral blood are essential components of immune microenvironment for the prediction of CRC metastasis. Moreover, exhausted T cells are characterized by higher expression of multiple inhibitory receptors, including PDCD1 and LAG3. Some genes such as PFKFB3, GNLY, circDCUN1D4, TXNIP and NR4A2 in T cells of cluster were statistically different between CRC metastasis and non-metastasis. The ligand-receptor interactions identified between different cluster cells and metastases-related DEGs identified from each cluster revealed that the communications of cells, alterations of functions, and numbers of T subsets may contribute to the metastasis of CRC. The mutation frequency of KiAA1551, ATP8B4 and LNPEP in T cells from tissues and SOR1 from peripheral blood were higher in metastatic CRC than that in non-metastatic CRC. In conclusion, the discovery of differential genes in T cells may provide potential targets for immunotherapy of CRC metastasis and relevant insights into the clinical prediction and prognosis of CRC metastasis.

1. Introduction

It was estimated that colorectal cancer (CRC), the third most frequent cancer and second leading cause of cancer-associated death worldwide, had 1.8 million new cases and 881,000 deaths in 2018 [1]. The main clinical manifestations of CRC include stomach aches,

* Corresponding author. No.1558, Sanhuan North Road, Wuxing District, Huzhou, Zhejiang Province, 313000, China.
E-mail address: ww@hzhospital.com (H. Zhao).
[1] These authors contributed equally to this work and should be considered co-first authors.

https://doi.org/10.1016/j.heliyon.2023.e17119
Received 16 March 2023; Received in revised form 1 June 2023; Accepted 7 June 2023
Available online 5 July 2023

bloody stools, and weight loss [2]. However, these symptoms are often overlooked at early stages of CRC, and more patients are likely to develop CRC metastasis at first diagnosis. About 20% of CRC patients develop metastasis, one of the main causes of CRC-associated death, accompanied by poor five-year prognosis [3]. The current study revealed that the regulation of epithelial to mesenchymal transition (EMT)-associated signaling pathway, such as WNT/β-catenin and TGF-β induced by abnormal expression of E-cadherin, N-cadherin, and vimentin, is responsible for CRC metastasis. In addition, alteration in a few gene biomarkers such as TP53, RAS, and BRAF, is responsible for the progression of CRC metastases [4,5]. However, for the complex process of metastasis, its underlying mechanisms are still poorly understood.

Cancer progression and metastasis are dependent on complex peripheral blood and tissue tumor microenvironments, the disruption of which may result in adverse consequences [6]. It has been proved that reduced lymphatic vessels and immune cytotoxicity of tumor microenvironment are important for the distant metastasis of CRC [7]. Primary tumors and metastases of CRC present a heterogeneous immune infiltration environment and an immune suppression microenvironment, which facilitates tumor immune escape and metastasis [7]. Cytokines or chemokines produced by immune infiltrating cells can both change tumor microenvironment and regulate the adaptive immune response to promote CRC metastasis [8]. T cell immunity comprises CD4+T cells, CD8+T cells, T Helper (TH) cells, and T regulatory (Treg) cells, and constitutes important components of the immune system as well. For example, tissue-resident memory CD8+T (TRM) cells was are related to lymph node metastasis and prognosis of tumors [9]. Some cytotoxic CD4+T cells can kill autologous tumors in an MHC-II dependent fashion and are suppressed by regulatory T cells [10]. T Helper (TH) cells are involved in the anti-tumor immune response [11]. The infiltration of high density Foxp3+Treg cells in the cancer tissues of CRC patients was is associated with a better prognosis [12]. The changes in T cell immunity in an immunological environment may induce immune escape mechanisms for the metastasis of CRC [13].

The treatment of CRC includes surgery, chemotherapy, radiotherapy, and so on. In recent years, immunotherapy, targeted therapy, and other cancer treatments have emerged, which provided new and effected treatments for cancer patients. As an innovative treatment, tumor immunotherapy has become a hot topic in the field of tumor therapy research. $CD8^+$ T cells play a key role and are significantly correlated with the prognosis of patients. For example, progression-free survival and overall survival are longer in CRC patients with cytotoxic $CD8^+$ T lymphocytes [14]. Immunocheckpoint inhibitor (ICI) treatment that rejuvenates T cells and modulate the adaptive immune system can prevent immune escape controlled by multiple checkpoints, such as cytotoxic T lymphocytes (CTL) associated protein 4 (CTLA-4) and programmed cell death ligand 1 (PD-L1) [15,16]. With a long-term effect on some patients with advanced cancer, immune checkpoint blockade (ICB) significantly improves the outcome of the disease [17]. However, immunotherapy currently provides little clinical benefits for 85% of CRC patients with pMMR and low microsatellite instability (MSI-L) or microsatellite stability (MSS) (PMMR-MSI-L/MSS) [18]. The prognosis of pMMR-MSI-L/MSS patients is worse than that of dMMR-MSI-H CRC [19]. In addition, several new drug combination regimens have emerged to provide more treatment options for patients with CRC. Brandi G et al. found that cytotoxic double- or triple-drug chemotherapy regiments (e.g. FOLFOX, FOLFOXIRI) after transplantation may be a safe approach for non-resettable colorectal liver metastases (NRCLM) patients receiving liver transplantation [20]. Viscardi G et al. evaluated the risk of early death from solid malignancies treated by immune checkpoint inhibitors alone or in combination with other drugs and discovered that ED after first-line ICI is a clinically relevant phenomenon of solid malignancies that could not be predicted by PD-L1 expression, but other treatments of ICI [21]. Regorafenib (REG) is an oral multikinase inhibitor in the treatment of CRC. A systematic review of 2,099 patients showed that the treatment with a standard dose of 160 mg of REG is associated with a significant increase in adverse events (adverse events)-related permanent withdrawal, dose interruption, and dose reduction [22]. However, the prognosis of CRC patients is not the same even when the tumor stage is the same, and the tumor heterogeneity of CRC remarkably affects the efficacy of immunotherapy. Therefore, in-depth exploration of the immune landscape of CRC may contribute to understanding the complexity of tumor heterogeneity, which may help design more appropriate therapies and develop new immunotherapy strategies.

Studies have indicated that gene mutation can change the copy number and function of related genes and lead to tumorigenesis. For instance, multiple RAS-related genes, including KRAS, NRAS and HRAS, are common mutated gene family in CRC. RAS mutation frequency is correlated with the invasion and metastasis of CRC [23]. What's more, mutations at sites 19 and 21 in EGFR gene are related to tumor genesis, progression and metastasis [24]. In addition, genetic mutations can alter the number and function of T cells. For example, mutations in the HER-2 gene affect the antigen recognition ability of T cells [25]. At present, there are relatively few studies on gene mutations in tumor infiltrating T cells, dominantly because the number of T cells isolated from the tumor tissue is insufficient. There is also great heterogeneity in each T cell subgroup. Single-cell RNA sequencing is a high-throughput experimental technique for quantifying gene expression profiles of specific cell populations by using RNA sequencing at the single-cell level. Meanwhile, it can evaluate the complex contribution of tumor genetic heterogeneity in multicellular organisms and different cell types [26]. Therefore, applying single-cell RNA sequencing to reveal the immune properties of T cells in the microenvironment surrounding the tumor is of great importance for cancer immunotherapy.

Until now, only the Zhang zemin group has detected the single T cell transcriptome profiling from CRC patients for determining the T cell properties and revealing tissue distribution of different T cells [27]. In their study, single T cell analysis by RNA sequencing and TCR tracking (STARTRAC) analysis was conducted to reveal the dynamic relationships of T cells in CRC. However, they did not explore metastasis-related mechanisms of T cell subsets in CRC. Thus, this study reclassified T cell cluster using unsupervised analysis and differential expression genes (DEGs) of each T cell cluster between non-metastatic and metastatic CRC samples from cancer tissues and peripheral blood. Besides, the possible biological functions and mutation frequencies of DEGs between non-metastatic and metastatic samples were investigated. The aim of this study was to provide new insights and treatment targets of metastasis at the single T cell genomic level.

2. Materials and methods

2.1. Data acquisition

The single-cell RNA sequencing data (GSE108989 dataset) were obtained from the Zhang zemin group. A total of 11,138 single T cells from 12 CRC patients were sequenced, among which 10,805 single T cells remained after data processing, including quality control, data filtration, and normalization. In this study, only processed transcriptomes of single T cells of 5 non-metastatic and 6 metastatic CRC samples from tissues and peripheral blood were used, with 3,003 T cells from peripheral blood and 4,656 T cells from cancer tissues. The cells were sequenced using Illumina HiSeq 4000 platform (Illumina, California, USA). The clinical characteristics of the 11 CRC samples are shown in Supp. Table 1.

2.2. Unsupervised clustering

Simpler single cell RNAseq data clustering (sscClust (https://github.com/Japrin/sscClust), package is a tool for multiple single cell RNAseq data analysis, including variable gene identification, dimension reduction, and clustering on reduced data [28]. In this study, sscClust package was used to sort T cells based on unsupervised clustering from cancer tissues and peripheral blood, respectively. First, the top 1,500 highly variable genes based on average expression and dispersion were selected, after which dimension reduction analysis was performed based on Spearman's correlation between cells. Afterwards, cell clustering was conducted by k-means algorithm, and a number of clusters were pre-established as 2–30. Subsequently, the final cluster classifications were determined by selecting the highest normalized mutual information (NMI) index and comparing the results of cell type identification shown in raw chip article [27]. Finally, the t-distributed stochastic neighbor embedding (t-SNE) method was adopted for cluster visualization.

2.3. Comparison of identified cell types with original article

Marker genes of T cell types identified in a previously published article [19] were reported (Supp.Table 2). Then, different T cell subtypes in each cluster were calculated. The main T cell types in each classified cluster were compared by unsupervised clustering. Finally, the violin plots of main T cell types in each cluster were drawn to validate our results.

2.4. Correlation analysis of clusters

Based on each defined cluster in cancer tissues and peripheral blood, and mean expression values of each gene in every cell type, the Pearson correlation coefficient among all the clusters were calculated using the cor function in R. Next, the corrplot software in R (https://mirrors.tuna.tsinghua.edu.cn/CRAN/web/packages/corrplot) [29] was applied to visualize the correlation heatmap.

2.5. Identifying cell type specific communication

To characterize T cell subset communications, the iTALK (https://github.com/Coolgenome/iTALK) package in R was used to explore cell communication by identifying ligand-receptor interactions among T cell subsets in cancer tissues and peripheral blood, respectively. On the one hand, the top 50% genes with high expression of each cluster were selected to explore ligand-receptor interactions between any two clusters and matched to the 2,648 known ligand-receptor interactions included in iTALK package, in which the genes were divided into 4 types: growth factor, cytokine, checkpoint, and others. On the other hand, on the bias of types of ligand genes and expression of ligand and receptor genes, each type of ligand-receptor interaction was ranked and ligand-receptor interaction networks were plotted and presented using the top 20 interactions of each type.

2.6. Differentially expressed gene (DEG) analysis

The differential expression of genes in each cluster between non-metastatic and metastatic CRC samples from cancer tissues and peripheral blood were analyzed using Bayesian methods in the limma package (Version 3.10.3, http://www.bioconductor.org/packages/2.9/bioc/html/limma.html) in R [30]. Afterwards, the p value was adjusted by Benjamini & Hochberg, and DEGs were screened by thresholds of adj.P.Val$<$0.05 and $|$log fold change (FC)$|>$1.

2.7. Functional and pathway enrichment analysis

Metascape (http://metascape.org) [31] is a powerful tool for providing functional enrichment, gene annotation, and membership search by integrating many functional biological databases, including Gene ontology (GO), Kyoto Encyclopedia of Genes and Genomes (KEGG), and Uniprot. In this study, the GO biological processes (BP) terms and KEGG pathways of DEGs of each cluster were analyzed under default parameters (Min Overlap: 3; P Value Cutoff: 0.01; Min Enrichment: 1.5). After obtaining terms that fit the given parameters, they were further clustered based on the similarity of genes enriched in each term larger than 0.3. The top 20 results of each cluster were presented using bar graph.

2.8. Protein-protein interaction (PPI) network analysis

Metascape tool was applied to identify PPI pairs of DEGs. The PPI enrichment analysis of DEGs was conducted using BioGrid [32], InWeb_IM [33], and OmniPath [34] databases under default parameters (Min Network Size: 3; Max Network Size: 500). After obtaining PPI pairs, the Cytoscape software (Version 3.4.0, http://chianti.ucsd.edu/cytoscape-3.4.0/) was used to construct and visualize the PPI network.

2.9. Comparison of mutation frequencies of DEGs between non-metastatic and metastatic samples

The somatic mutation files of SNP calling of non-metastatic and metastatic COAD and READ samples were downloaded from the TCGA database (https://tcga-data.nci.nih.gov/). Then, the gene mutation frequency of DEGs identified from each cluster in non-metastatic and metastatic COAD and READ samples were counted using maftools software (Version 2.0.16) in R [35].

3. Results

3.1. Distinct T cell clusters identified from tissue and peripheral blood

Under pre-setting 2–30 clusters, the overall T cell population from tissue and peripheral blood were classified using unsupervised k-means clustering, respectively. The NMI index corresponding to different cluster numbers is shown in Fig. 1A and B. Since the NMI indexes were the highest when the number of clusters were 8 and 4 for tumor and peripheral blood-derived T cells, respectively, a total of 8 tumor T cell clusters and 4 peripheral blood T cell clusters were identified. The t-SNE plots demonstrated distinct clusters from

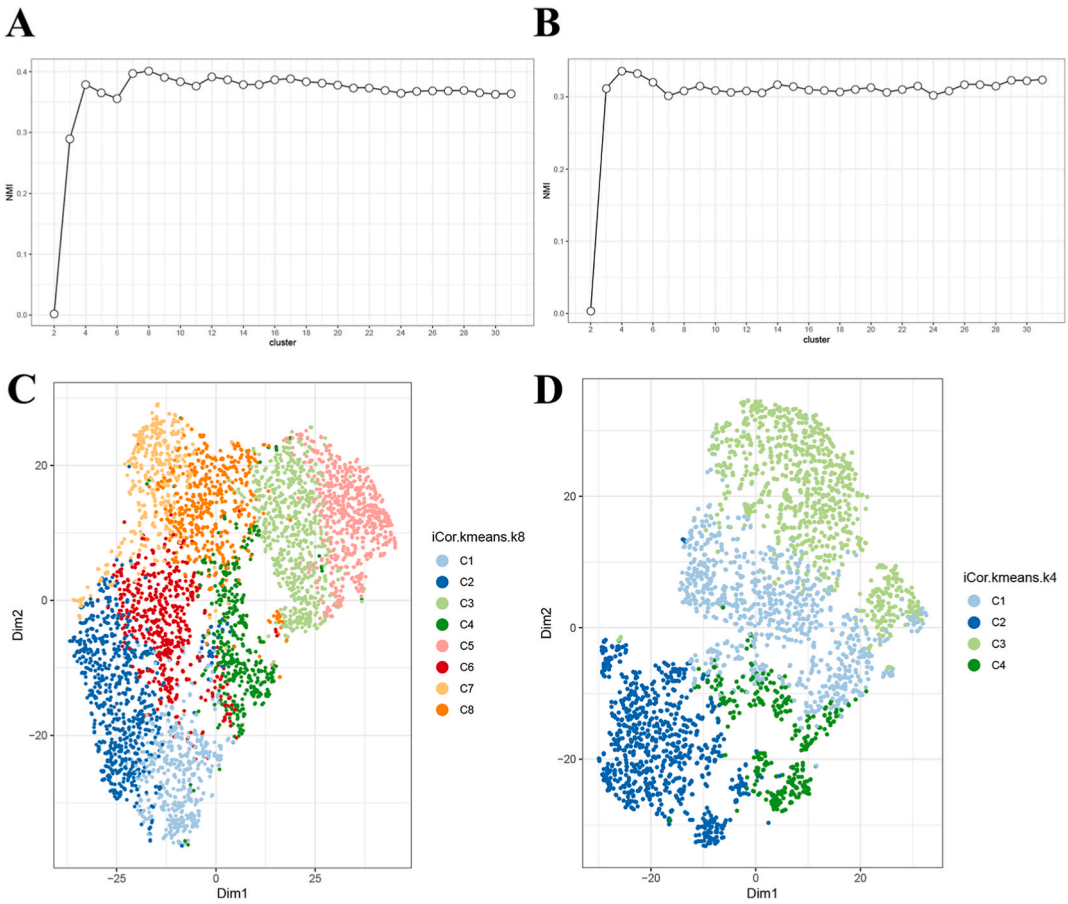

Fig. 1. Identification of distinct T cell clusters from CRC tumor tissue and peripheral blood. A) A total of 8 clusters of T cell populations from CRC tumor tissue emerged using unsupervised clustering. B) A total of 4 clusters of T cell populations from CRC peripheral blood emerged using unsupervised clustering. The number of clusters was chosen when the corresponding NMI index was the highest. X-axis represents the number of k-means clusters, while Y-axis represents the corresponding NMI index. NMI: normalized mutual information. C) tSNE plots show 8 distinct clusters of T cells from CRC tumor tissue. D) tSNE plots show 4 distinct clusters of T cells from CRC peripheral blood. Different colors refer to different T cell clusters. (For interpretation of the references to color in this figure legend, the reader is referred to the Web version of this article.)

tumor T cells (Fig. 1C) and distinct clusters from peripheral blood T cells (Fig. 1D).

3.2. Characteristics of T cell subtypes composition of each cluster

The number of T cell subtypes of each cluster from tumor and peripheral blood samples was calculated based on marker genes of each T cell subtype provided by an original article (http://crc.cancer-pku.cn/) (Supp.Tables 3 and 4). A total of 4,656 cells were composed of 8 tumor T cells clusters, and Tumor-T regulatory cells (Tumor-Treg) (1192) made up a major proportion of all the cells (25.6%), followed by exhausted CD8+T cells (CD8+TEX) cells (15.6%). CD8+TEX cells were most abundant T cell populations in cluster 1 (C1). Effector memory CD8+T cells (CD8+TEM) and CD8+TEX were both dominant in C2. Tumor-Treg cells were dominant in C3 and C5, TH1-like T cells were most dominant in C4, CD8+TEM were most dominant in C6, while resident memory CD4+T cells (CD4+TRM) were dominant in C7 and C8 (Supp.Table 3). These were further validated by violin plots, which showed the expressions of gene markers for CD8+TEX, CD8+TEM, Tumor-Treg, TH1-like T cells, and CD4+TRM in the 8 clusters from tumor T cells (Fig. 2).

In 4 peripheral blood clusters, 3003 cells were identified, and CD8+terminal differentiated effector memory (CD8+TEMRA/TEFF, 638) was the most abundant T cell subset, accounting for 21.2% of all cells. CD4+blood-central memory T cells (CD4+blood-TCM) and blood-Treg were dominant in C1; CD4+blood-TCM and CD8+TEMRA/TEFF were dominant in C2; CD4+TN were dominant in C3; CD4+TEMRA/TEFF were dominant in C4 (Supp.Table 4). Moreover, the violin plots exhibited a distinct expression distribution of gene markers for $CD4^{+}$ blood-TCM, blood-Treg, CD8+TEMRA/TEFF, and naive CD4+T cell (CD4+TN) in the 4 clusters (Fig. 2).

3.3. Significant correlation of different clusters in CRC T cell subtypes

Among the 8 tissue clusters, the correlation of T cell subsets of C3 and C5 with other clusters was relatively weak, but there was a significant positive correlation between the two clusters. In addition, apparent positive correlations existed between C7 and C8, C6 and C2, and C1 and C2. C7 had a significantly negative correlation with most clusters (C1-5) (Fig. 3A).

In 4 peripheral blood clusters, all the clusters had positive correlations, and apparent positive correlations existed between C1 and C3, C1 and C4, and C2 and C4 (Fig. 3B).

The heterogeneity within Treg and Trm subsets differs between non-metastatic and metastatic CRC. The venn analysis showed that there were 76 differential genes in Treg (C3 and C5) subgroups and 68 differential genes in Trm (C7 and C8) subgroups between the

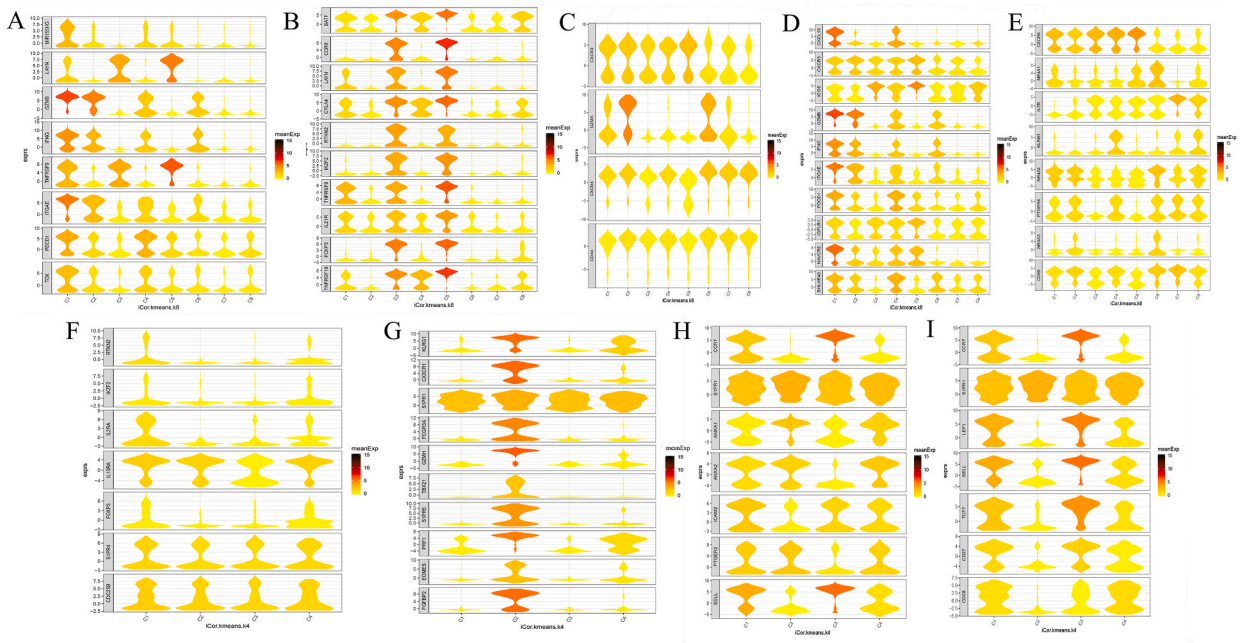

Fig. 2. Violin plots show expressions comparison of selected genes markers for cluster. Violin plots show genes marker expressions for CD8+TEX (A), Tumor-Treg (B), CD8+TEM (C), TH1-like T cells (D), and CD4+TRM (E) in 8 clusters from tumor T cells, and blood-Treg (F), CD8+TEMRA/TEFF (G), CD4+blood-TCM (H) and naive CD4+T cell (I) in 4 clusters from peripheral blood T cells, respectively. The color of each violin represents the average expression value of a given gene in each cell cluster. The change of color from yellow to black represents the average expression value from the lowest to the highest score.

CD8+TEX: exhausted CD8+T cells; Treg: T regulatory cell; CD8+TEMRA/TEFF: CD8+terminal differentiated effector memory. CD8+TEM: Effector memory CD8+T cells; TH1-like T cells: T helper 1-like T cells, CD4+TRM: resident memory CD4+T cells; CD4+blood-TCM: CD4+Peripheral blood-central memory T cells; CD4+TN: naive CD4+T cell. (For interpretation of the references to color in this figure legend, the reader is referred to the Web version of this article.)

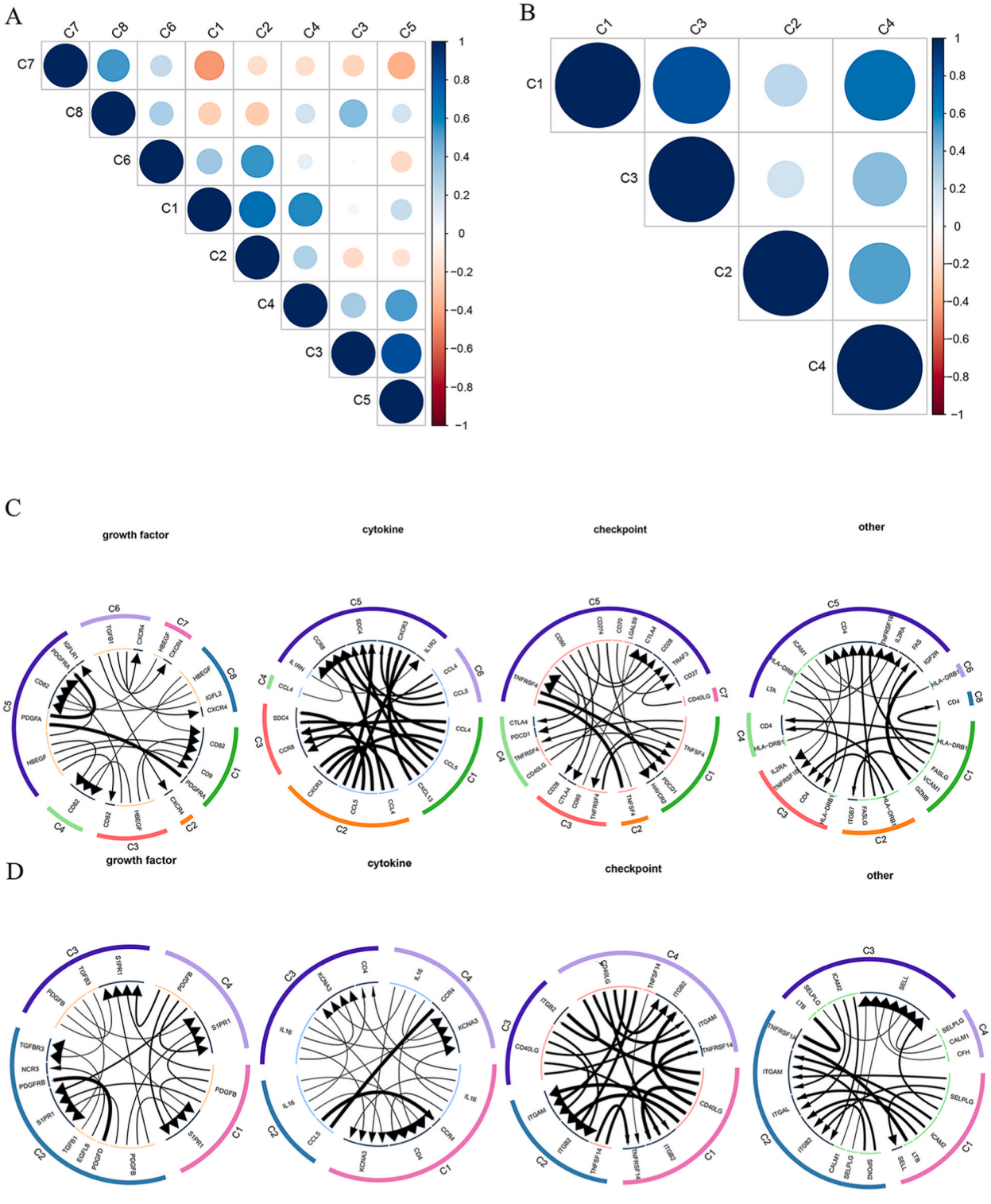

(caption on next page)

Fig. 3. Correlation analyses of different clusters and analysis of cell-cell communications by excavating ligand-receptor interactions among clusters. A) Correlation heatmap of clusters from tumor tissue T cells. Apparent positive correlations exist between clusters 7 and 8, clusters 6 and 2, and clusters 1 and 2. B) Correlation heatmap of clusters from peripheral blood T cells. There are positive correlations between clusters 1 and 3, clusters 1 and 4, and clusters 2 and 4. The color gradient from dark blue to red represents the highest positive correlations to highest negative correlations ($r = 1$ to $r = -1$). The size of nodes is proportional to the absolute value of the correlation coefficient. C) The top 20 ligand-receptor interaction pairs for growth factor type, cytokine type, checkpoint type, and other types of clusters from tumor tissue T cells. D) The top 20 ligand-receptor interaction pairs for growth factor type, cytokine type, checkpoint type, and other types of clusters from peripheral blood T cells. Different colors in the outer circle represent different cell clusters, while colors in inner circle represent different gene types. Arrows indicate the receptor, and the size of the arrow is proportional to receptor expression level, while the thickness of the line is proportional to ligand expression level. The line links the receptor in one cell cluster to a ligand in another cell cluster. (For interpretation of the references to color in this figure legend, the reader is referred to the Web version of this article.)

metastatic and non-metastatic groups (Supplemental Fig. 1). The list of different genes was showed in Supp. Tables 5 and 6.

3.4. Ligand-receptor interactions among clusters in CRC T cell subtypes

The communications among tissue and peripheral blood T subsets were explored by excavating ligand-receptor pairs among clusters. A total of 8,681 ligand-receptor pairs were obtained from tissue T cell subsets include 688 pairs of growth factor type, 1,108 pairs of cytokine type, 451 pairs of checkpoint type, and 6,434 pairs of other type. The top 20 ligand-receptor pairs of each type are shown in Fig. 3C. Many of the highest-expression interactions were found in the chemokine type. The highly expressed receptor CCR8, a gene marker of tumor-Treg, was detected in C3 and C5. The ligand CCL4 highly expressed in C1 and C2 had both receptor CCR8 in C3 and C5.

Furthermore, a group of 1,349 ligand-receptor pairs was obtained from peripheral blood T subsets, including 72 pairs of growth factor type, 123 pairs of cytokine type, 37 pairs of checkpoint type, and 1,117 pairs of other type. The top 20 ligand-receptor pairs of each type are shown in Fig. 3D. The most highly expressed interactions belonged to the 'other' type, including SELPLG-SELL, ICAM2-ITGB2, and LTB-TNFRSF1A.

3.5. Differences for T cell subsets between metastatic and non-metastatic CRC

First, the total T cells from tissue-derived and peripheral blood-derived metastatic non-metastatic CRC samples were calculated (Table 1). There were increasing trends of overall T cell counts in non-metastatic samples compared with metastatic samples from each cluster, except peripheral blood C4. The number of T cells from tissue identified in clusters showed a greater difference between C2 and C7, but there were no obvious differences among the other clusters (Table 1A). The number of overall T cells from peripheral blood C4 was significantly lower than that from C1, C2, and C3 (Table 1B), which revealed the tissue or microenvironment preferences of different T subsets.

Furthermore, the number of each main T cell subset was counted from metastatic and non-metastatic samples, respectively (Table 2). As a result, high CD8+TEX, CD4+TRM, tumor-Treg, TH1-like T, and CD8+TEM cell counts were found in tissue-derived metastatic samples compared with non-metastatic samples, especially tumor-Treg from C3 and CD4+TRM from C7 (Table 2A). Meanwhile, significantly higher levels of CD4+TN were found in peripheral blood-derived metastatic samples rather than in non-metastatic samples (Table 2B). The DEGs of each cluster between T cells from metastatic and non-metastatic cancer tissues and peripheral blood samples were identified. A total of 282 DEGs between tissues-derived T cells were screened, including 39, 37, 51, 66, 25, 60, 28, and 40 DEGs from C1, C2, C3, C4, C5, C6, C7, and C8, respectively, among which 28 (e.g., LAG3) were specific in C1, 21 were specific in C2, 26 were specific in C3, 47 were specific in C4, 14 were specific in C5, 43 were specific in C6, 19 were specific in C7, and 33 were specific in C8. GNLY and PHLDA were specifically upregulated in C4. Three common DEGs (PDCD1, PFKFB3, and FAM46C) were only identified in C1 and C2, while several DEGs (DUSP10, HIVEP1, AOAH, SNX9, PMAIP1, and UBE2B) were only identified in C3 and C5.

In addition, a total of 153 DEGs between peripheral blood-derived T cells were screened, including 36, 31, 25, and 89 from C1, C2, C3, and C4. A total of 22, 18, 12, and 81 DEGs were specifically deregulated in C1, C2, C3, and C4, respectively. Among these DEGs, TXNIP, NR4A2, and ZNF331 were identified in 4 clusters. JAML was only significantly upregulated in C2 and C4. Moreover, several DEGs (e.g., HLA-DMA, HLA-DRB5, HLA-DRB1, and HLA-DQA1) were identified only in C4. The heatmaps for DEGs for cancer tissues and peripheral blood derived clusters are shown in Fig. 4.

Table 1
The counts of total T cells from tissue-derived (A) and peripheral blood-derived (B) metastatic and non-metastatic CRC samples.

A	Clusters	C1	C2	C3	C4	C5	C6	C7	C8
	Non-metastasis	212	282	173	201	302	278	116	191
	Metastasis	314	492	524	249	356	308	309	348
B	Clusters	C1	C2	C3	C4				
	Non-metastasis	379	395	336	168				
	Metastasis	513	412	636	164				

Table 2
The counts of most abundance T cell subset in each cluster tissue-derived (A) and peripheral blood-derived (B) metastatic and non-metastatic CRC samples.

	T cell subset	Clusters	Metastasis	Non-metastasis	Counts
A	CD8 C07-LAYN	C1	237	176	413
	CD8 C07-LAYN	C2	171	98	269
	CD8 C04-GZMK	C2	156	145	301
	CD4 C12-CTLA4	C3	407	112	519
	CD4 C09-CXCL13	C4	106	66	172
	CD4 C12-CTLA4	C5	331	269	600
	CD8 C04-GZMK	C6	145	47	192
	CD4 C05-CXCR6	C7	112	30	142
	CD4 C05-CXCR6	C8	63	49	112
B	CD4 C10-FOXP3	C1	123	83	206
	CD4 C02-ANXA1	C1	179	120	299
	CD8 C03-CX3CR1	C2	285	279	564
	CD4 C01-CCR7	C3	245	117	362
	CD8 C03-CX3CR1	C4	2	70	72

3.6. Functions of DEGs in CRC T cell subtypes between metastatic and non-metastatic CRC

The DEGs in 8 clusters from tissue and 4 clusters from peripheral blood were subjected to functional enrichment analyses. For tissue-derived DEGs, the DEGs were totally enriched in 307 GO BP terms and 32 KEGG pathways. Based on clustering of similarity terms or pathways, 20 representative terms or pathways were obtained (Fig. 5A). The DEGs from all clusters except for cluster 1 were most significantly enriched on GO BP term "T cell activation", while all clusters except for cluster 2 were enriched in "positive regulation of cell death". Five clusters (C2, C3, C4, C6, and C8) involved in "cytokine-mediated signaling pathway", "leukocyte activation involved in immune response", and "leukocyte migration" were significantly associated with C2 and C8. The "T cell co-stimulation" GO term was only associated with C2. The pathway of "Cell adhesion molecules (CAMs)" was significantly enriched in C7 and C8.

For DEGs from peripheral blood, the DEGs were completely involved in 307 GO BP terms and 32 KEGG pathways. Twenty representative terms or pathways were presented in Fig. 5B. The GO BP terms, "cytokine-mediated signaling pathway" and "lymphocyte activation" in all clusters, "adaptive immune response" in C1, C3 and C4, and "leukocyte activation involved in immune response" in C1–C3, and the pathways of "Epstein-Barr virus infection" were significantly enriched in all clusters. Interesting, the GO terms, "cell chemotaxis" and "negative regulation of immune system process" were only significantly enriched in C4.

PPI networks of DEGs of each cluster in CRC T cell subtypes between metastatic and non-metastatic CRC.

The DEGs of each cluster were used to construct the PPI network, and the nodes and PPI pairs in the PPI network of each cluster from tissue (Table 3A) and peripheral blood (Table 3B) were counted. For tissue-derived cluster, the PPI network of C6 had the most nodes, in which several heat shock protein family members, HSP90AA1, HSPB1, HSPD1, HSPA1B, and HSPA1A had more interactions (Fig. 5C). For peripheral blood derived cluster, the PPI network of C4 had the most nodes, JUN and MYC were highlighted in this network, and a subnetwork with most major histocompatibility complex family members, including HLA-DMA, HLA-DRB5, HLA-DRB1, and HLA-DQA1, were obtained (Fig. 5D).

3.7. Mutation frequencies of DEGs between non-metastatic and metastatic CRC

From TCGA database, the somatic mutation data of 233 metastatic and 296 non-metastatic samples from colon and rectal cancer were obtained. In non-metastatic and metastatic CRC cancer samples, the gene mutation frequencies of most DEGs identified from each cluster did not show great differences, while a few had obvious differences. KIAA1551 and ATP8B4 were both exclusively expressed in tissue C4 and the gene mutation frequencies of KIAA1551 and ATP8B4 were 1% vs 6% and 0% vs 6% between metastatic and non-metastatic samples, respectively. In tissue C8, LNPEP was also specially expressed, and the gene mutation frequencies of LNPEP were 0% vs 5% (Fig. 5E). SORL1 that was exclusively expressed in peripheral blood C4 had 1% mutation frequency in metastatic CRC

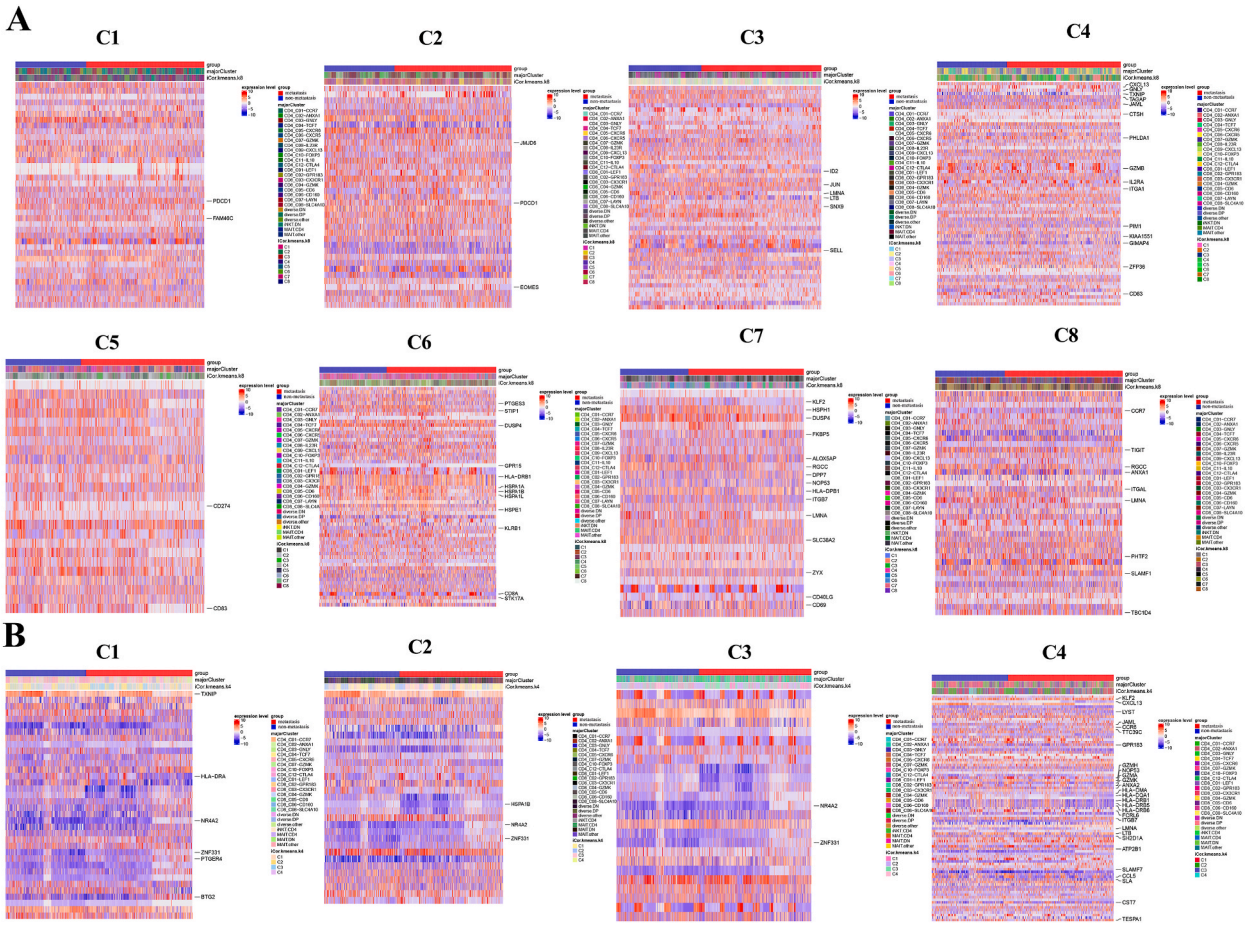

Fig. 4. Heatmaps of differentially expressed genes (DEGs) in-between CRC metastatic and non-metastatic samples from tumor tissue and peripheral blood.

A) Heatmaps of DEGs in C1–C8 between CRC metastatic and non-metastatic samples from tumor tissue. B) Heatmaps of DEGs in C1, C2, C3, and C4 between CRC metastatic and non-metastatic samples from peripheral blood.

The genes with |logFC| >1.5 are marked. The blue color in the X-axis is the non-metastatic samples, while red in the X-axis marks the metastatic samples. The color gradient from blue to red represents the express changes of downregulation to upregulation. (For interpretation of the references to color in this figure legend, the reader is referred to the Web version of this article.)

cancer and 8% mutation frequency in non-metastatic CRC cancer (Fig. 5F). The results suggested that the frequency of gene mutation of T cells in the metastatic samples was lower than that in the non-metastatic samples.

3.8. Ligand-receptor interactions for T cell subsets between metastatic and non-metastatic CRC

DEGs in CRC T cell subtypes between metastatic and non-metastatic CRC were used to further analyze the communications by excavating ligand-receptor pairs. The top 20 ligand-receptor pairs of 4 clusters from peripheral blood and 8 clusters from tissue are shown in Fig. 6A and B, respectively. In the T cell from peripheral blood, the highly expressed receptor CXCR3 was detected in C1, C2 and C4, the highly expressed receptor ITGB1 was detected in C1 and C3, and the highly expressed receptor SELL was detected in C2 and C3 from peripheral blood. The highly expressed interactions included IL16-CD4, IL16-KCNA3 in C2 and C3, and CXCL13-CXCR3 in C1 and C4. In the T cell subsets from tissues, the highly expressed receptors were CCR1 and CXCR3 in C1 and C2. The most highly expressed interactions included CCL5-CCR1, CCL5-CXCR3, CXCL13-CXCR3, and CXCL13-CXCR5 in C1 and C2. Thus, these receptors, including CXCR3, ITGB1 and SELL in T cell subsets from peripheral blood, and CCR1 and CXCR3 in T cell subsets from tissues were associated with CRC metastasis.

4. Discussion

Treating cancer metastasis is usually more difficult for its uncontrollability, and tumor microenvironment is a critical determinant for distant metastasis, which elucidates the underlying mechanisms during metastasis, especially in tumor microenvironment is of

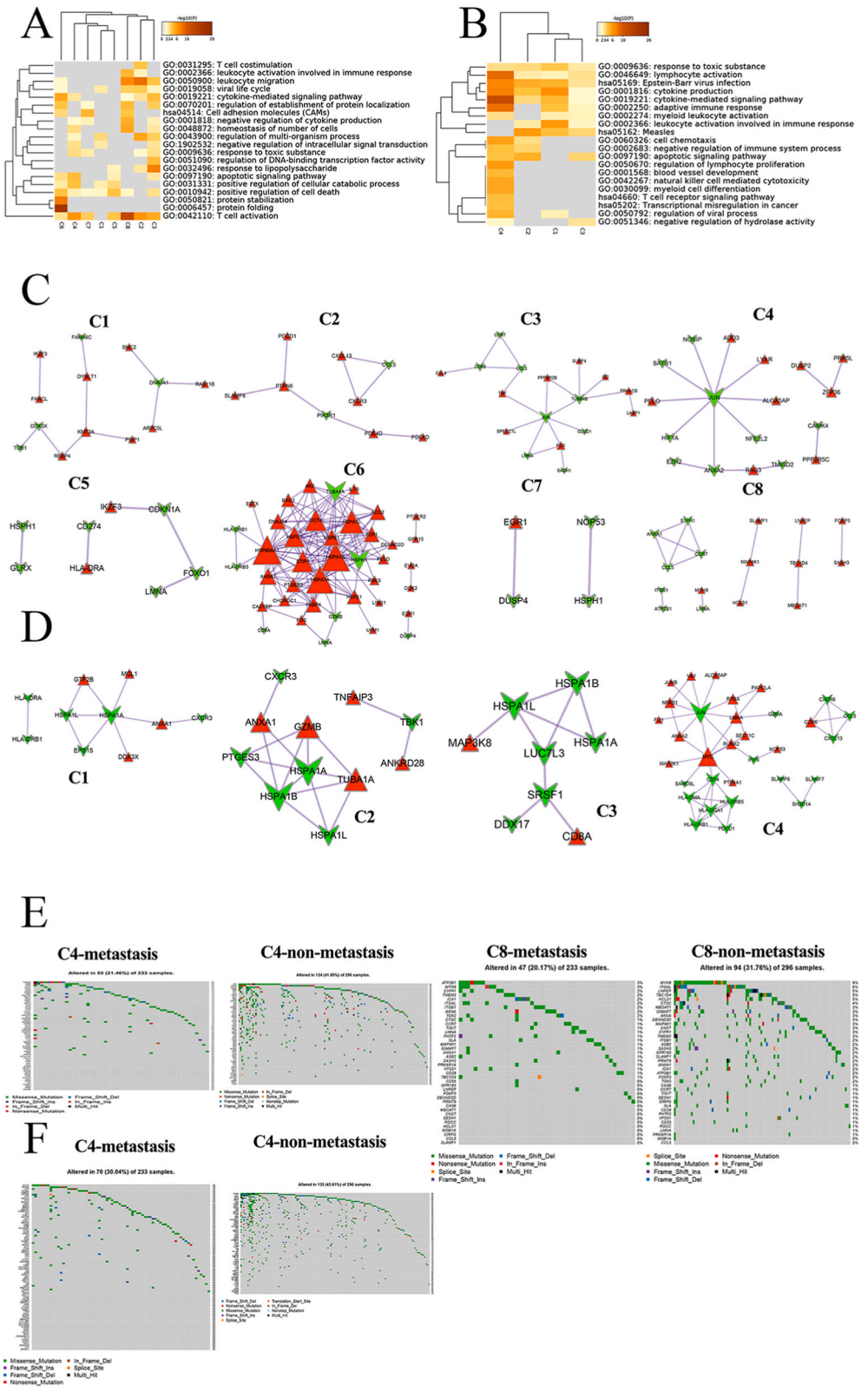

(caption on next page)

Fig. 5. Functional enrichment results for the DEGs identified between CRC metastatic and non-metastatic samples in each cluster, PPI network for DEGs between CRC metastatic and non-metastatic samples in each cluster, and comparison of mutation frequencies of DEGs between non-metastatic and metastatic samples. A) The clustergram shows top 20 representative terms or pathways for DEGs from tumor tissue. B) The clustergram shows top 20 representative terms or pathways for DEGs from peripheral blood. X-axis represents different cell clusters, while Y-axis presents the terms of biological processes or pathways. The darker the color is, the smaller the p value is. C) PPI network for DEGs in tumor tissue derived cluster. D) PPI network for DEGs in peripheral blood derived cluster. Red and triangle nodes represent the up-regulated genes, while green V-shaped nodes represent the down-regulated genes. The size of node is proportional to the degree values of the node itself. E) Oncoplots show mutation frequencies of DEGs in tumor tissue derived C4 and C8, counted by 233 metastatic and 296 non-metastatic samples of colon and rectum cancer from the TCGA database. F) Oncoplots show mutation frequencies of DEGs in peripheral blood derived C4 counted by 233 metastatic and 296 non-metastatic samples of colon and rectum cancer from the TCGA database. (For interpretation of the references to color in this figure legend, the reader is referred to the Web version of this article.)

Table 3
Attribute statistics of PPI network of each cluster from cancer tissues (A) and peripheral blood (B).

A	cluster	node	edge
	C1	13	10
	C2	9	8
	C3	17	19
	C4	18	15
	C5	8	5
	C6	40	144
	C7	4	2
	C8	16	13
B	C1	10	10
	C2	11	17
	C3	8	9
	C4	32	47

great importance [36]. In this study, unsupervised clustering was used to identify new T cell clusters on the bias of previous single-cell RNA sequencing data, and the annotation of the identified clusters was conducted. High CD8+TEX, CD4+TRM, tumor-Treg, and TH1-like T cell counts were found in tissue-derived metastatic samples, and significantly higher levels of CD4+TN were found in peripheral blood-derived metastatic samples rather than non-metastatic samples. Furthermore, the biological interpretation and DEGs of each cluster in terms of metastasis were analyzed. These findings may offer potential targets for CRC metastasis immunotherapy and provide related insights for CRC metastasis prediction and prognosis in clinic.

Single RNA sequencing identified 4655 T cells from tissue and 3003 T cells from peripheral blood. Tumor-Treg cells (1192, 25.6%) were most abundant in overall tissue T cell populations followed by exhausted CD8+T cells, while CD8+TEMRA/TEFF (638, 21.2%) was most abundant T cell subset in peripheral blood, which revealed the heterogeneities of T cells from different sources. In addition, it was found that CD8+TEX, CD4+TRM, TH1-like T cells, tumor-Treg, and CD8+TEM from tissue, and CD4+TN from peripheral blood were higher in metastatic samples than non-metastatic samples. Tregs are a kind of important T cell subset for peripheral tolerance and restraining autoimmunity responses. An interesting study proved that the increase of tumor-infiltrating Tregs may facilitate metastasis development of pancreatic cancer by establishing an immunosuppressive microenvironment, while reduced Tregs may suppress metastasis formation [37]. The accumulation of tumor-associated Tregs is critical in suppressing auto-tumor specific T cell responses in liver cancer and CRC liver metastases, thus leading to immune evasion [38]. CD8+TEX is named as exhausted T cells that present with the loss of effector functions, and it could potentially accelerate progression or deterioration of the cancer [39]. Reportedly, breast cancer patients with a high percentage of T exhaustion markers are likely to develop the progressive types, such as metastatic inflammatory [40]. In addition, the elevated CD4+naïve/memory ratio reflects the progression of pancreatic cancer and is associated with poorer clinical response and prognosis [41]. Moreover, the circulating lower CD4+TN cells are detected in response to post-stereotactic body radiotherapy in lung metastasis [42]. Our results demonstrated that CD8+TEX, CD4+TRM, TH1-like T cells, CD8+TEM, and tumor-Treg from tissue, and CD4+TN from peripheral blood that function as essential components of immune microenvironment are potential biomarkers for CRC metastasis prediction.

The results of correlation analysis indicated that there were significant positive correlations between C1 and C2, C3 and C5, C6 and C2, and C7 and C8 from tissue, as well as between C1 and C3, C1 and C4, and C2 and C4 from peripheral blood. It was inferred that these results might be associated with similarity of T cell subsets of each cluster. In tissue-derived clusters, CD8+TEX cells were most abundant in cluster 1 and in C2 as a main T cell subtype. In addition, the highest dominance of Tumor-Treg was in clusters 3 and 5, CD8+TEM in C2 and C6, and CD4+TRM in C7 and C8. Ligand-receptor interaction between cells is a main type of cell communication. In this study, several significant ligand-receptor interactions between different clusters were screened, and the highest scoring pairwise interaction was the ligand CCL4 from C1 and C2, and their shared receptor CCR8 from C3 and C5. CCR8, as a chemokine receptor, is mainly expressed in Tregs and can regulate the antitumor immunity in tumor microenvironment [43]. Notably, the CD8+T cells with CCL4 expression had lower potential for immune reconstitution [44]. In peripheral blood derived clusters, it was also found that SELL, a receptor of C3, had more interactions with ligands from other clusters. Selectin L (SELL), an adhesion/homing receptor, is necessary for CD4+TN cell extravasation from peripheral blood to peripheral lymph nodes [45]. Also, circulating lower naïve CD4+T cells are

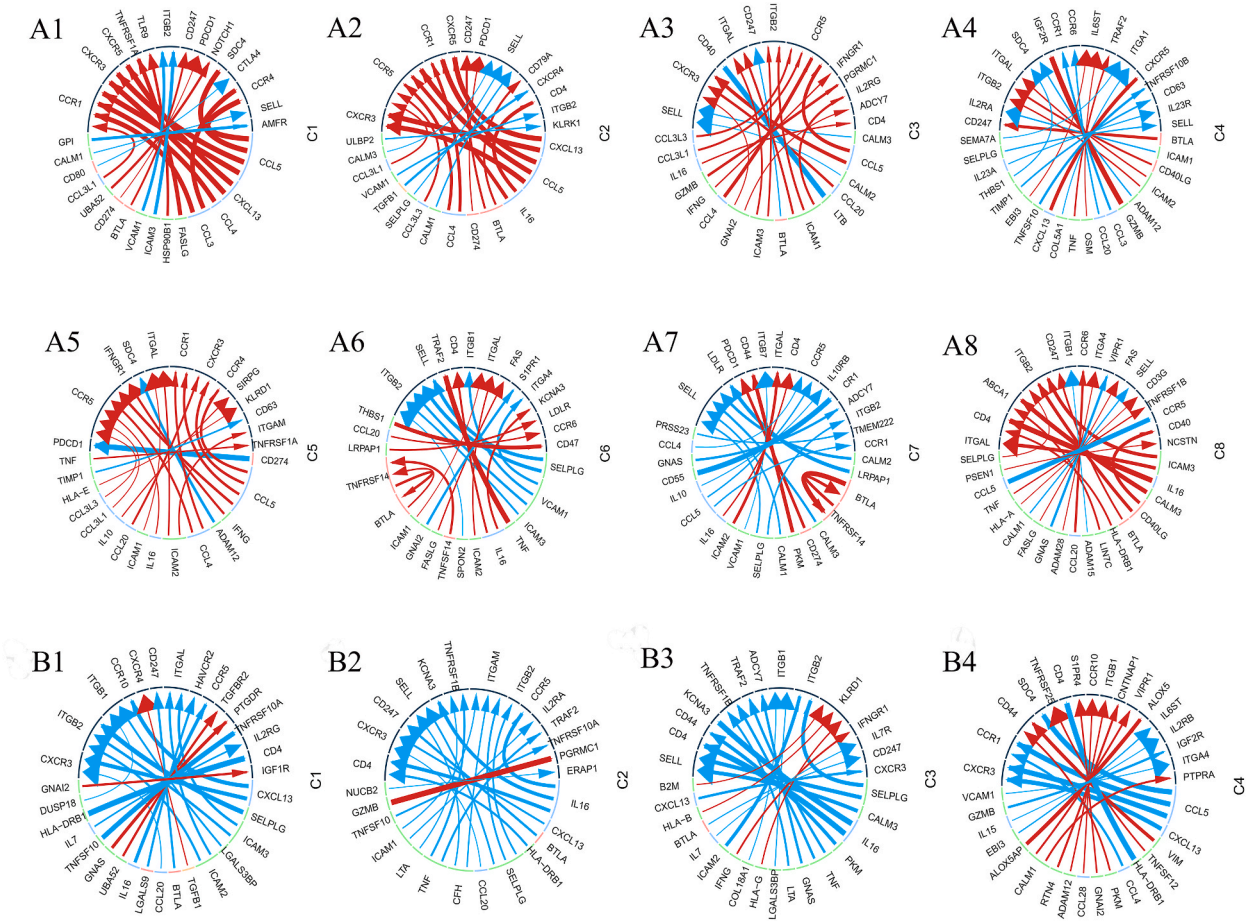

Fig. 6. Ligand-receptor interactions for T cell subsets between metastatic and non-metastatic CRC. A1-A8) The top 20 ligand-receptor interaction pairs for growth factor type, cytokine type, checkpoint type, and other types of clusters from tumor tissue T cells. B1–B4) The top 20 ligand-receptor interaction pairs for growth factor type, cytokine type, checkpoint type, and other types of clusters from peripheral blood T cells. Different colors in the outer circle represent different cell clusters, while colors in inner circle represent different gene types. Arrows indicate the receptor, and the size of the arrow is proportional to receptor expression level, while the thickness of the line is proportional to ligand expression level. The red arrow represents the Gain relationship, while the blue arrow stands for the Loss relationship. The line links the receptor in one cell cluster to a ligand in another cell cluster. (For interpretation of the references to color in this figure legend, the reader is referred to the Web version of this article.)

positively corrected with distant metastatic spread of cancer [46]. Moreover, our study proved that SELL, as DEG identified from peripheral blood C3, was downregulated in naïve CD4+T cells from CRC metastases samples. Taken together, the development and metastases of CRC may be co-regulated by different T cell subsets through ligand-receptor interaction communications with each other.

Furthermore, the similarities and differences of molecular expression between metastasis and non-metastasis samples were analyzed, and several common and specific DEGs among different clusters were identified. For tissue-derived clusters, LAG3 was specifically upregulated in C1, and GNLY and PHLDA were specifically upregulated in tissue C4. Three common DEGs, namely PDCD1, PFKFB3, and FAM46C, were only specifically identified in C1 and C2 (exhausted CD8+T cells), while other DEGs (eg., DUSP10, HIVEP1, AOAH, SNX9, PMAIP1, and UBE2B) were only specifically identified in C3 and C5. Reportedly, exhausted T cells are characterized by higher expression of multiple inhibitory receptors (eg., PDCD1 and LAG3) [47], which is consistent with our results. For peripheral blood derived clusters, the DEGs TXNIP, NR4A2, and ZNF331 were identified in all clusters, and DEGs [eg., HLA-DMA (MHC Class II Antigen DMA), HLA-DRB5, HLA-DRB1 (MHC Class II HLA-DR Beta 1 Chain), and HLA-DQA1] were only identified in C4. The differential expression of these genes in T cells may simultaneously affect the functions and number of T subsets to contribute to the metastasis of CRC.

This study identified PFKFB3 of C1 and GNLY of C4 in tissues and NR4A2 and TXNIP of C1 in peripheral blood from metastatic and non-metastatic CRC. PFKFB3 did not affect cancer cell proliferation but could inhibit cancer metastasis [48]. The upregulation of PFKFB3 promoted PD-L1 expression in T cells and reduced the function of cytotoxic T cells [49]. GNLY (granulosin) secreted by cytotoxic T lymphocytes played an important anti-cancer role by inducing apoptosis [50]. Low expression of GNLY in

tumor-infiltrating effector memory T cells was associated with metastasis and poor prognosis in CRC [51]. circDCUN1D4 inhibited the metastasis of lung adenocarcinoma by stabilizing TXNIP expression [52]. TXNIP deficiency increased the function of effector T cells but did not affect T cell development and homeostasis [53]. NR4A2 deficiency can regulate the aggravation of colitis by regulating Treg cells and affecting the function of Th1 cells [54]. NR4A2 regulated CRC invasion, metastasis, and poor prognosis through Wnt/β-catenin pathway [55]. Our findings are consistent with these relevant studies. In conclusion, the discovery of differential genes in T cells may provide potential targets for immunotherapy of CRC metastasis and relevant insights for clinical prediction and prognosis of CRC metastasis.

Additionally, it was found that DEGs from most tissue and peripheral blood-derived clusters were both closely associated with "cytokine-mediated signaling pathway" and "leukocyte activation involved in immune response". Cytokine-mediated signals can differentially regulate T cell behavior, which is pivotal for the control of immune responses [56]. PPI analysis showed that Jun/Myc signaling pathway in peripheral blood C4 (CD4+TEMRA/TEFF) was associated with CRC metastasis. An interesting study results [57] showed that Myc was a negative regulatory factor and could effectively inhibit CRC cell invasion and migration. What's more, the high expression of c-Myc in colorectal cancer was positively correlated with cancer metastasis [58]. Reportedly, Myc can promote CD4 + T cell proliferation by down-regulating microRNA-451A [59]. Therefore, it was concluded that the up-regulation of Jun/Myc pathway in CD4+TEMRA/TEFF could reduce the number of CD4+TEMRA/TEFF and inhibit immune function, which suggested that Jun/Myc might involve in the T cell regulation of CRC metastasis.

Additionally, the numbers and activities of T lymphocytes may influence immunocompetence [60], and the co-effecters of immunocompetence and immunosuppression of immune response may be responsible for cancer metastasis [61]. These findings revealed the importance of the two main functions during the progression of CRC. Current studies [62] showed that increased Treg cell frequency in tumors is associated with disease progression and poor prognosis in cancer patients. The study revealed that DEGs, including CD274 andCD83 in C5, were enriched in "T cell activation" and "positive regulation of cell death" in the metastatic group, which was consistent with relevant studies. The results indicated that DEGs in C5 can affect CRC metastasis through activating Treg cell and promoting Treg cells proliferation. In the present study, it was found that adhesion signaling pathways in T cells were also related to metastasis. Adhesion signaling pathways are involved in cancer metastasis. In the present study, adhesion signaling pathways in T cells were also related to metastasis, which is an interesting discovery. Whether the metastasis of cancer cells is accompanied by the metastasis of immune cells is a topic worthy of further exploration. The "negative regulation of immune system process" was enriched in the C4 cluster, which means that this cluster takes on a more Treg phenotype. The "Epstein-Barr virus infection" pathway was related to tumor T cell responses. Some specific genes, such as NR4A2, ZNF331, TXNIP and JAML, might be associated with poor immune control of metastasis.

Most studies on genetic mutations focused on cancer cells, but relatively few studies focused on genetic mutations in immune cells. It was found that the frequency of gene mutation of T cells in the metastatic samples was lower than that in the non-metastatic samples. It is speculated that the frequency of gene mutation in T cells could affect cancer metastasis. The frequency of gene mutation in T cells can provide a potential predictive marker for cancer metastasis.

This study provides evidence for the similarities and differences on infiltrating T subsets of tissue or peripheral blood derived from different clusters at both cellular and molecular levels, which may offer potential targets for the immunotherapy of CRC progression. Although only 5 non-metastatic and 6 metastatic CRC samples from both tissues and peripheral blood were analyzed in this study, the transcriptomes of single T cells of 3,003 T cells from peripheral blood and 4,656 T cells from cancer tissues were also included. Therefore, the sample size was sufficient for our subsequent analysis, as each individual cell amounted to one sample. In addition, despite the previous definitions of T cell subset, all the T cells obtained from samples were re-classified into different clusters using unsupervised clustering based on different algorithms. Unsupervised clustering is a powerful tool for identifying the putative T cell types [63].

5. Conclusion

T cell subsets isolated from CRC tumor tissue and peripheral blood metastasis and non-metastasis samples were clustered, and it showed that significant heterogeneity existed in the infiltrating T cell clusters. The high levels of CD8+TEX, CD4+TRM, TH1-like T cells, CD8+TEM, and tumor-Treg from tissue, and CD4+TN from peripheral blood may be essential components of immune microenvironment for the prediction of CRC metastasis. Moreover, exhausted T cells are characterized by higher expression of multiple inhibitory receptors, including PDCD1 and LAG3. Some genes such as PFKFB3, GNLY, circDCUN1D4, TXNIP and NR4A2 in T cells of cluster are statistically different between CRC metastasis and non-metastasis. The ligand-receptor interactions identified between different cluster cells and metastases related DEGs identified from each cluster revealed that the communications of cells, alterations of functions, and numbers of T subsets may contribute to the metastasis of CRC. The mutation frequency of KiAA1551, ATP8B4 and LNPEP in T cells from tissues and SOR1 from peripheral blood were higher in metastatic CRCs than that in non-metastatic CRCs. In conclusion, the discovery of differential genes in T cells may provide potential targets for immunotherapy of CRC metastasis and relevant insights for clinical prediction and prognosis of CRC metastasis.

Declarations

Author contribution statement

Zhuang Jing, Qu Zhanbo: Analyzed and interpreted the data; Wrote the paper.

Chu Jian, Ru Lixin: Contributed reagents, materials, analysis tools or data; Wrote the paper.
Wang Jingjing, Wu Yinhang: Analyzed and interpreted the data.
Fan Zhiqing, Song Yifei: Contributed reagents, materials, analysis tools or data.
Han Shuwen, Zhao Hui: Conceived and designed the experiments.

Ethics approval and consent to participate

Not applicable.

Funding statement

Jing Zhuang was supported by Zhejiang Medical and Health Technology Project {2021KY343, 2022KY1220}, Public Welfare Technology Application Research Program of Huzhou {2020GY01}.

Data availability statement

Data will be made available on request.

Declaration of competing interest

The authors declare that they have no known competing financial interests or personal relationships that could have appeared to influence the work reported in this paper.

Acknowledgements

The authors gratefully acknowledge the database available to us for this study.

Appendix A. Supplementary data

Supplementary data to this article can be found online at https://doi.org/10.1016/j.heliyon.2023.e17119.

References

[1] F. Bray, J. Ferlay, I. Soerjomataram, R.L. Siegel, L.A. Torre, A. Jemal, Global cancer statistics 2018: GLOBOCAN estimates of incidence and mortality worldwide for 36 cancers in 185 countries, CA A Cancer J. Clin. 68 (6) (2018) 394–424.
[2] K. Alvarez, A. Cassana, M. De La Fuente, T. Canales, M. Abedrapo, F. López-Köstner, Clinical, pathological and molecular characteristics of Chilean patients with early-, intermediate- and late-onset colorectal cancer, Cells 10 (3) (2021).
[3] D.V. Tauriello, A. Calon, E. Lonardo, E. Batlle, Determinants of metastatic competency in colorectal cancer, Mol. Oncol. 11 (1) (2017) 97–119.
[4] R. Yaeger, W.K. Chatila, M.D. Lipsyc, J.F. Hechtman, A. Cercek, F. Sanchez-Vega, G. Jayakumaran, S. Middha, A. Zehir, M.T.A. Donoghue, et al., Clinical sequencing defines the genomic landscape of metastatic colorectal cancer, Cancer Cell 33 (1) (2018) 125–136.e123.
[5] M.K.C. Lee, J.M. Loree, Current and emerging biomarkers in metastatic colorectal cancer, Curr. Oncol. 26 (Suppl 1) (2019) S7–s15.
[6] D.F. Quail, J.A. Joyce, Microenvironmental regulation of tumor progression and metastasis, Nat. Med. 19 (11) (2013) 1423–1437.
[7] M. Van den Eynde, B. Mlecnik, G. Bindea, T. Fredriksen, S.E. Church, L. Lafontaine, N. Haicheur, F. Marliot, M. Angelova, A. Vasaturo, et al., The link between the multiverse of immune microenvironments in metastases and the survival of colorectal cancer patients, Cancer Cell 34 (6) (2018) 1012–1026.e1013.
[8] M. Pancione, G. Giordano, A. Remo, A. Febbraro, L. Sabatino, E. Manfrin, M. Ceccarelli, V. Colantuoni, Immune escape mechanisms in colorectal cancer pathogenesis and liver metastasis, J. Immun. Res. 2014 (2014), 686879.
[9] J.J. Milner, C. Toma, B. Yu, K. Zhang, K. Omilusik, A.T. Phan, D. Wang, A.J. Getzler, T. Nguyen, S. Crotty, et al., Runx3 programs CD8(+) T cell residency in non-lymphoid tissues and tumours, Nature 552 (7684) (2017) 253–257.
[10] D.Y. Oh, S.S. Kwek, S.S. Raju, T. Li, E. McCarthy, E. Chow, D. Aran, A. Ilano, C.S. Pai, C. Rancan, et al., Intratumoral CD4(+) T cells mediate anti-tumor cytotoxicity in human bladder cancer, Cell 181 (7) (2020) 1612–1625.e1613.
[11] R. Purwar, C. Schlapbach, S. Xiao, H.S. Kang, W. Elyaman, X. Jiang, A.M. Jetten, S.J. Khoury, R.C. Fuhlbrigge, V.K. Kuchroo, et al., Robust tumor immunity to melanoma mediated by interleukin-9-producing T cells, Nat. Med. 18 (8) (2012) 1248–1253.
[12] W.H. Fridman, J. Galon, F. Pagès, E. Tartour, C. Sautès-Fridman, G. Kroemer, Prognostic and predictive impact of intra- and peritumoral immune infiltrates, Cancer Res. 71 (17) (2011) 5601–5605.
[13] X. Huang, Y. Zou, L. Lian, X. Wu, X. He, X. He, X. Wu, Y. Huang, P. Lan, Changes of T cells and cytokines TGF-β1 and IL-10 in mice during liver metastasis of colon carcinoma: implications for liver anti-tumor immunity, J. Gastrointest. Surg. 17 (7) (2013) 1283–1291.
[14] J. Galon, A. Costes, F. Sanchez-Cabo, A. Kirilovsky, B. Mlecnik, C. Lagorce-Pagès, M. Tosolini, M. Camus, A. Berger, P. Wind, et al., Type, density, and location of immune cells within human colorectal tumors predict clinical outcome, Science 313 (5795) (2006) 1960–1964.
[15] P. Sharma, J.P. Allison, Dissecting the mechanisms of immune checkpoint therapy, Nat. Rev. Immunol. 20 (2) (2020) 75–76.
[16] P. Sharma, B.A. Siddiqui, S. Anandhan, S.S. Yadav, S.K. Subudhi, J. Gao, S. Goswami, J.P. Allison, The next decade of immune checkpoint therapy, Cancer Discov. 11 (4) (2021) 838–857.
[17] H. Borghaei, L. Paz-Ares, L. Horn, D.R. Spigel, M. Steins, N.E. Ready, L.Q. Chow, E.E. Vokes, E. Felip, E. Holgado, et al., Nivolumab versus docetaxel in advanced nonsquamous non-small-cell lung cancer, N. Engl. J. Med. 373 (17) (2015) 1627–1639.
[18] A.J. Franke, W.P. Skelton, J.S. Starr, H. Parekh, J.J. Lee, M.J. Overman, C. Allegra, T.J. George, Immunotherapy for colorectal cancer: a review of current and novel therapeutic approaches, J. Natl. Cancer Inst. 111 (11) (2019) 1131–1141.

[19] D.T. Le, J.N. Uram, H. Wang, B.R. Bartlett, H. Kemberling, A.D. Eyring, A.D. Skora, B.S. Luber, N.S. Azad, D. Laheru, et al., PD-1 blockade in tumors with mismatch-repair deficiency, N. Engl. J. Med. 372 (26) (2015) 2509–2520.

[20] G. Brandi, A.D. Ricci, A. Rizzo, C. Zanfi, S. Tavolari, A. Palloni, S. De Lorenzo, M. Ravaioli, M. Cescon, Is post-transplant chemotherapy feasible in liver transplantation for colorectal cancer liver metastases? Cancer Commun. 40 (9) (2020) 461–464.

[21] G. Viscardi, A.C. Tralongo, F. Massari, M. Lambertini, V. Mollica, A. Rizzo, F. Comito, R. Di Liello, S. Alfieri, M. Imbimbo, et al., Comparative assessment of early mortality risk upon immune checkpoint inhibitors alone or in combination with other agents across solid malignancies: a systematic review and meta-analysis, Eur. J. Cancer 177 (2022) 175–185.

[22] A. Rizzo, M. Nannini, M. Novelli, A. Dalia Ricci, V.D. Scioscio, M.A. Pantaleo, Dose reduction and discontinuation of standard-dose regorafenib associated with adverse drug events in cancer patients: a systematic review and meta-analysis, Ther. Adv. Med. Oncol. 12 (2020), 1758835920936932.

[23] T. Yoshino, D.C. Portnoy, R. Obermannová, G. Bodoky, J. Prausová, R. Garcia-Carbonero, T. Ciuleanu, P. García-Alfonso, A.L. Cohn, E. Van Cutsem, et al., Biomarker analysis beyond angiogenesis: RAS/RAF mutation status, tumour sidedness, and second-line ramucirumab efficacy in patients with metastatic colorectal carcinoma from RAISE-a global phase III study, Ann. Oncol. 30 (1) (2019) 124–131.

[24] R. Bhargava, W.L. Gerald, A.R. Li, Q. Pan, P. Lal, M. Ladanyi, B. Chen, EGFR gene amplification in breast cancer: correlation with epidermal growth factor receptor mRNA and protein expression and HER-2 status and absence of EGFR-activating mutations, Mod. Pathol. 18 (8) (2005) 1027–1033.

[25] J.R. Veatch, B.L. Jesernig, J. Kargl, M. Fitzgibbon, S.M. Lee, C. Baik, R. Martins, A.M. Houghton, S.R. Riddell, Endogenous CD4(+) T cells recognize neoantigens in lung cancer patients, including recurrent oncogenic KRAS and ERBB2 (Her2) driver mutations, Canc. Immun. Res. 7 (6) (2019) 910–922.

[26] T. Baslan, J. Hicks, Unravelling biology and shifting paradigms in cancer with single-cell sequencing, Nat. Rev. Cancer 17 (9) (2017) 557–569.

[27] L. Zhang, X. Yu, L. Zheng, Y. Zhang, Y. Li, Q. Fang, R. Gao, B. Kang, Q. Zhang, J.Y. Huang, et al., Lineage tracking reveals dynamic relationships of T cells in colorectal cancer, Nature 564 (7735) (2018) 268–272.

[28] X. Guo, Y. Zhang, L. Zheng, C. Zheng, J. Song, Q. Zhang, B. Kang, Z. Liu, L. Jin, R. Xing, et al., Global characterization of T cells in non-small-cell lung cancer by single-cell sequencing, Nat. Med. 24 (7) (2018) 978–985.

[29] Wei T SV: R Package "Corrplot": Visualization of a Correlation Matrix (Version 0.84).

[30] A. Colaprico, T.C. Silva, C. Olsen, L. Garofano, C. Cava, D. Garolini, T.S. Sabedot, T.M. Malta, S.M. Pagnotta, I. Castiglioni, et al., TCGAbiolinks: an R/Bioconductor package for integrative analysis of TCGA data, Nucleic Acids Res. 44 (8) (2016) e71.

[31] Y. Zhou, B. Zhou, L. Pache, M. Chang, A.H. Khodabakhshi, O. Tanaseichuk, C. Benner, S.K. Chanda, Metascape provides a biologist-oriented resource for the analysis of systems-level datasets, Nat. Commun. 10 (1) (2019) 1523.

[32] C. Stark, B.J. Breitkreutz, T. Reguly, L. Boucher, A. Breitkreutz, M. Tyers, BioGRID: a general repository for interaction datasets, Nucleic Acids Res. 34 (Database issue) (2006) D535–D539.

[33] T. Li, R. Wernersson, R.B. Hansen, H. Horn, J. Mercer, G. Slodkowicz, C.T. Workman, O. Rigina, K. Rapacki, H.H. Stærfeldt, et al., A scored human protein-protein interaction network to catalyze genomic interpretation, Nat. Methods 14 (1) (2017) 61–64.

[34] D. Türei, T. Korcsmáros, J. Saez-Rodriguez, OmniPath: guidelines and gateway for literature-curated signaling pathway resources, Nat. Methods 13 (12) (2016) 966–967.

[35] A. Mayakonda, D.C. Lin, Y. Assenov, C. Plass, H.P. Koeffler, Maftools: efficient and comprehensive analysis of somatic variants in cancer, Genome Res. 28 (11) (2018) 1747–1756.

[36] L. Yang, P.C. Lin, Mechanisms that drive inflammatory tumor microenvironment, tumor heterogeneity, and metastatic progression, Semin. Cancer Biol. 47 (2017) 185–195.

[37] J.A. Kenkel, W.W. Tseng, M.G. Davidson, L.L. Tolentino, O. Choi, N. Bhattacharya, E.S. Seeley, D.A. Winer, N.E. Reticker-Flynn, E.G. Engleman, An immunosuppressive dendritic cell subset accumulates at secondary sites and promotes metastasis in pancreatic cancer, Cancer Res. 77 (15) (2017) 4158–4170.

[38] A. Pedroza-Gonzalez, C. Verhoef, J.N. Ijzermans, M.P. Peppelenbosch, J. Kwekkeboom, J. Verheij, H.L. Janssen, D. Sprengers, Activated tumor-infiltrating CD4+ regulatory T cells restrain antitumor immunity in patients with primary or metastatic liver cancer, Hepatology 57 (1) (2013) 183–194.

[39] M. Kurachi, CD8(+) T cell exhaustion, Semin. Immunopathol. 41 (3) (2019) 327–337.

[40] S. Adams, S. Loi, D. Toppmeyer, D.W. Cescon, M. De Laurentiis, R. Nanda, E.P. Winer, H. Mukai, K. Tamura, A. Armstrong, et al., Pembrolizumab monotherapy for previously untreated, PD-L1-positive, metastatic triple-negative breast cancer: cohort B of the phase II KEYNOTE-086 study, Ann. Oncol. 30 (3) (2019) 405–411.

[41] J. Hang, J. Huang, S. Zhou, L. Wu, Y. Zhu, L. Zhu, H. Zhou, K. Xu, H. Jiang, X. Yang, The clinical implication of CD45RA(+) naïve T cells and CD45RO(+) memory T cells in advanced pancreatic cancer: a proxy for tumor biology and outcome prediction, Cancer Med. 8 (3) (2019) 1326–1335.

[42] C. Liu, Q. Hu, B. Xu, X. Hu, H. Su, Q. Li, X. Zhang, J. Yue, J. Yu, Peripheral memory and naïve T cells in non-small cell lung cancer patients with lung metastases undergoing stereotactic body radiotherapy: predictors of early tumor response, Cancer Cell Int. 19 (2019) 121.

[43] D.O. Villarreal, A. L'Huillier, S. Armington, C. Mottershead, E.V. Filippova, B.D. Coder, R.G. Petit, M.F. Princiotta, Targeting CCR8 induces protective antitumor immunity and enhances vaccine-induced responses in colon cancer, Cancer Res. 78 (18) (2018) 5340–5348.

[44] R. Casetti, C. Pinnetti, A. Sacchi, G. De Simone, V. Bordoni, E. Cimini, N. Tumino, F. Besi, D. Viola, F. Turchi, et al., HIV-specific CD8 T cells producing CCL-4 are associated with worse immune reconstitution during chronic infection, J. Acquir. Immune Defic. Syndr. 75 (3) (2017) 338–344.

[45] L.M. Bradley, S.R. Watson, S.L. Swain, Entry of naive CD4 T cells into peripheral lymph nodes requires L-selectin, J. Exp. Med. 180 (6) (1994) 2401–2406.

[46] Y.Y. Wang, N. Zhou, H.S. Liu, X.L. Gong, R. Zhu, X.Y. Li, Z. Sun, X.H. Zong, N.N. Li, C.T. Meng, et al., Circulating activated lymphocyte subsets as potential blood biomarkers of cancer progression, Cancer Med. 9 (14) (2020) 5086–5094.

[47] P. Jönsson, J.H. Southcombe, A.M. Santos, J. Huo, R.A. Fernandes, J. McColl, M. Lever, E.J. Evans, A. Hudson, V.T. Chang, et al., Remarkably low affinity of CD4/peptide-major histocompatibility complex class II protein interactions, Proc. Natl. Acad. Sci. U. S. A. 113 (20) (2016) 5682–5687.

[48] A.R. Cantelmo, L.C. Conradi, A. Brajic, J. Goveia, J. Kalucka, A. Pircher, P. Chaturvedi, J. Hol, B. Thienpont, L.A. Teuwen, et al., Inhibition of the glycolytic activator PFKFB3 in endothelium induces tumor vessel normalization, impairs metastasis, and improves chemotherapy, Cancer Cell 30 (6) (2016) 968–985.

[49] D.P. Chen, W.R. Ning, Z.Z. Jiang, Z.P. Peng, L.Y. Zhu, S.M. Zhuang, D.M. Kuang, L. Zheng, Y. Wu, Glycolytic activation of peritumoral monocytes fosters immune privilege via the PFKFB3-PD-L1 axis in human hepatocellular carcinoma, J. Hepatol. 71 (2) (2019) 333–343.

[50] L. Martinez-Lostao, D. de Miguel, S. Al-Wasaby, A. Gallego-Lleyda, A. Anel, Death ligands and granulysin: mechanisms of tumor cell death induction and therapeutic opportunities, Immunotherapy 7 (8) (2015) 883, 882.

[51] F. Pagès, A. Berger, M. Camus, F. Sanchez-Cabo, A. Costes, R. Molidor, B. Mlecnik, A. Kirilovsky, M. Nilsson, D. Damotte, et al., Effector memory T cells, early metastasis, and survival in colorectal cancer, N. Engl. J. Med. 353 (25) (2005) 2654–2666.

[52] Y. Liang, H. Wang, B. Chen, Q. Mao, W. Xia, T. Zhang, X. Song, Z. Zhang, L. Xu, G. Dong, et al., circDCUN1D4 suppresses tumor metastasis and glycolysis in lung adenocarcinoma by stabilizing TXNIP expression, Mol. Ther. Nucleic Acids 23 (2021) 355–368.

[53] J. Muri, H. Thut, M. Kopf, The thioredoxin-1 inhibitor Txnip restrains effector T-cell and germinal center B-cell expansion, Eur. J. Immunol. 51 (1) (2021) 115–124.

[54] T. Sekiya, I. Kashiwagi, N. Inoue, R. Morita, S. Hori, H. Waldmann, A.Y. Rudensky, H. Ichinose, D. Metzger, P. Chambon, et al., The nuclear orphan receptor Nr4a2 induces Foxp3 and regulates differentiation of CD4+ T cells, Nat. Commun. 2 (2011) 269.

[55] Y.F. Han, G.W. Cao, Role of nuclear receptor NR4A2 in gastrointestinal inflammation and cancers, World J. Gastroenterol. 18 (47) (2012) 6865–6873.

[56] W. Huang, A. August, The signaling symphony: T cell receptor tunes cytokine-mediated T cell differentiation, J. Leukoc. Biol. 97 (3) (2015) 477–485.

[57] X. Ma, J. Huang, Y. Tian, Y. Chen, Y. Yang, X. Zhang, F. Zhang, L. Xue, Myc suppresses tumor invasion and cell migration by inhibiting JNK signaling, Oncogene 36 (22) (2017) 3159–3167.

[58] W. Wang, J. Deng, Q. Wang, Q. Yao, W. Chen, Y. Tan, Z. Ge, J. Zhou, Y. Zhou, Synergistic role of Cul1 and c-Myc: prognostic and predictive biomarkers in colorectal cancer, Oncol. Rep. 38 (1) (2017) 245–252.

[59] Z. Zeng, K. Wang, Y. Li, N. Xia, S. Nie, B. Lv, M. Zhang, X. Tu, Q. Li, T. Tang, et al., Down-regulation of microRNA-451a facilitates the activation and proliferation of CD4(+) T cells by targeting Myc in patients with dilated cardiomyopathy, J. Biol. Chem. 292 (14) (2017) 6004–6013.

[60] R. Nagatomi, The implication of alterations in leukocyte subset counts on immune function, Exerc. Immunol. Rev. 12 (2006) 54–71.
[61] A. Adler, J.A. Stein, S. Ben-Efraim, Immunocompetence, immunosuppression, and human breast cancer. II. Further evidence of initial immune impairment by integrated assessment effect of nodal involvement (N) and of primary tumor size (T), Cancer 45 (8) (1980) 2061–2073.
[62] M. Ahmadzadeh, A. Pasetto, L. Jia, D.C. Deniger, S. Stevanović, P.F. Robbins, S.A. Rosenberg, Tumor-infiltrating human CD4(+) regulatory T cells display a distinct TCR repertoire and exhibit tumor and neoantigen reactivity, Sci. Immun. 4 (31) (2019).
[63] V.Y. Kiselev, T.S. Andrews, M. Hemberg, Challenges in unsupervised clustering of single-cell RNA-seq data, Nat. Rev. Genet. 20 (5) (2019) 273–282.